



# Sintering behavior and microwave dielectric properties of High-Q $\text{Li}_2(\text{Mg}_{1-x}\text{Zn}_x)_3\text{Ti}(\text{O}_{0.96}\text{F}_{0.08})_6$ ceramics for LTCC application

Ping Zhang\*, Manman Hao, Xin Tian, Sheng Xie\*

School of Electrical and Information Engineering, School of Microelectronics and Key Laboratory of Advanced Ceramics and Machining Technology of Ministry of Education, Tianjin University, Tianjin 300072, PR China

## ARTICLE INFO

### Article history:

Received 10 June 2021

Received in revised form 6 July 2021

Accepted 7 July 2021

Available online 8 July 2021

### Keywords:

$\text{Li}_2(\text{Mg}_{1-x}\text{Zn}_x)_3\text{Ti}(\text{O}_{0.96}\text{F}_{0.08})_6$

High-Q

Microwave dielectric properties

Low temperature co-fired ceramic

## ABSTRACT

$\text{Li}_2(\text{Mg}_{1-x}\text{Zn}_x)_3\text{Ti}(\text{O}_{0.96}\text{F}_{0.08})_6$  (LMZTF) ceramics were fabricated through the solid-state reaction method. All samples diffraction peaks belong to  $\text{Zn}_2\text{TiO}_4$  and  $\text{Li}_2\text{Mg}_3\text{TiO}_6$ . The SEM characterization and bulk density testing demonstrated the uniform microstructure of LMZTF ceramics. In this work, the dielectric loss of  $\text{Li}_2\text{Mg}_3\text{Ti}(\text{O}_{0.96}\text{F}_{0.08})_6$  ceramics was greatly reduced through ion doping. The High-Q  $\text{Li}_2(\text{Mg}_{0.98}\text{Zn}_{0.02})_3\text{Ti}(\text{O}_{0.96}\text{F}_{0.08})_6$  ceramics sintered at 950 °C for 6 h possessed outgoing microwave dielectric properties:  $\epsilon_r \sim 14.64$ ,  $Q \times f \sim 128,000$  GHz,  $\tau_f \sim -33.9$  ppm/°C, which made it a promising candidate for low temperature co-fired ceramic (LTCC) applications.

© 2021 Elsevier B.V. All rights reserved.

## 1. Introduction

Microwave dielectric ceramics have excellent characteristics such as low loss, high resonance frequency stability, and low production costs [1–3]. Quality factor ( $Q \times f$  values), dielectric constant ( $\epsilon_r$ ) and temperature stability ( $\tau_f$ ) are the important evaluation criteria of microwave ceramics [4,5]. The commonly used silver electrode layer has a melting point of 961 °C. Therefore, ceramic materials with excellent dielectric performance that can be co-fired with Ag or Cu electrodes at low temperatures are an important research object in the current era [6–11].

It has been reported that Li-based ceramics such as  $\text{Li}_2\text{MgTiO}_4$ ,  $\text{Li}_2\text{MgTi}_3\text{O}_8$ , and  $\text{Li}_2\text{Mg}_3\text{TiO}_6$  exhibit the advantages of adjustable dielectric constant and ultra-low dielectric loss [12–14]. In 2015, Fu et al. [14] explored the  $\text{Li}_2\text{Mg}_3\text{TiO}_6$  ceramics. In 2016, Zhang et al. [15] reported the effects of  $\text{Ni}^{2+}$ ,  $\text{Ca}^{2+}$ ,  $\text{Mn}^{2+}$ , and  $\text{Zn}^{2+}$  on dielectric properties of  $\text{Li}_2\text{Mg}_3\text{TiO}_6$  ceramics. Among them,  $\text{Li}_2(\text{Mg}_{0.95}\text{Zn}_{0.05})_3\text{TiO}_6$  ceramics possessed excellent microwave properties. Then, the impact of the non-stoichiometric ratio on the properties of  $\text{Li}_2\text{Mg}_3\text{TiO}_6$  ceramics was discussed.  $\text{Li}_2\text{Mg}_{3.6}\text{TiO}_{6.6}$  ceramics sintered at 1375 °C obtained outgoing properties [16].  $\text{Co}^{2+}$  was used to replace  $\text{Mg}^{2+}$  to systematically analyze the influences of crystal structure on the performance of

$\text{Li}_2\text{Mg}_3\text{TiO}_6$  ceramics [17]. Wu et al. [18,19] used composite ions ( $\text{Mg}_{1/3}\text{Sb}_{2/3}$ )<sup>4+</sup> and ( $\text{Mg}_{1/3}\text{Nb}_{2/3}$ )<sup>4+</sup> to replace  $\text{Ti}^{4+}$  ions of  $\text{Li}_2\text{Mg}_3\text{TiO}_6$  ceramics.  $\text{Li}_2\text{Mg}_3\text{Ti}_{0.95}(\text{Mg}_{1/3}\text{Nb}_{2/3})_{0.05}\text{O}_6$  ceramics sintered at 1575 °C for 4 h possessed outgoing microwave dielectric properties:  $\epsilon_r \sim 14.79$ ,  $Q \times f \sim 204,900$  GHz,  $\tau_f \sim -18.43$  ppm/°C. In 2017, Xie et al. [11] used  $\text{Ca}_{0.8}\text{Sr}_{0.2}\text{TiO}_3$  to improve the  $\tau_f$  value of  $\text{Li}_2\text{Mg}_3\text{TiO}_6$  ceramics. When the composition was  $0.9\text{Li}_2\text{Mg}_3\text{TiO}_6\text{--}0.09\text{Ca}_{0.8}\text{Sr}_{0.2}\text{TiO}_3$ , the value of  $\tau_f$  was  $-3.65$  ppm/°C.

However, there are few studies on the low-temperature sintering of  $\text{Li}_2\text{Mg}_3\text{TiO}_6$  ceramics. In 2017, Fu et al. [20] used LiF as a sintering aid and  $\text{Ca}_{0.8}\text{Sr}_{0.2}\text{TiO}_3$  as a  $\tau_f$  compensator to successfully prepare a dielectric material that met the requirements of LTCC technology. The sintering temperature of the  $\text{Li}_6\text{Mg}_7\text{Ti}_3\text{O}_{16} + 4$  wt%LiF,  $\text{Li}_2\text{Mg}_3\text{SnO}_6 + 5$  wt%LiF and  $\text{Li}_2\text{Mg}_3\text{TiO}_6 + 4$  wt%LiF ceramics was reduced to below 950 °C and the ceramics had satisfactory dielectric properties [21–23]. Liu et al. [24] reported that  $\text{Mg}_{0.85}\text{Zn}_{0.15}\text{SiO}_3$  ceramics obtained outgoing dielectric properties when sintered at 1360 °C. In addition, compared with other ions, the  $\text{F}^-$  ion has excellent chemical stability. Therefore, replacing  $\text{O}^{2-}$  ion with  $\text{F}^-$  ion can reduce the sintering temperature of  $\text{Li}_2\text{Mg}_3\text{TiO}_6$  ceramics and maintain its outgoing dielectric properties [25]. Since the radius of  $\text{Zn}^{2+}$  ions is similar to  $\text{Mg}^{2+}$  ions, the  $\text{Mg}^{2+}$  ions in  $\text{Li}_2\text{Mg}_3\text{TiO}_6$  ceramics can be replaced by  $\text{Zn}^{2+}$  ions. Appropriate amounts of  $\text{Zn}^{2+}$  replacing  $\text{Mg}^{2+}$  may have a positive impact on the performance of the  $\text{Li}_2\text{Mg}_3\text{Ti}(\text{O}_{0.96}\text{F}_{0.08})_6$  ceramics.

In this paper, the  $\text{Mg}^{2+}$  ions in  $\text{Li}_2(\text{Mg}_{1-x}\text{Zn}_x)_3\text{Ti}(\text{O}_{0.96}\text{F}_{0.08})_6$  (LMZTF) were replaced by different contents of  $\text{Zn}^{2+}$  ions. The

\* Corresponding authors.

E-mail addresses: [zptai@163.com](mailto:zptai@163.com) (P. Zhang), [xie\\_sheng06@tju.edu.cn](mailto:xie_sheng06@tju.edu.cn) (S. Xie).

change law of microstructure and dielectric properties were researched. Finally, LMZTF ( $0.02 \leq x \leq 0.08$ ) ceramics with excellent properties and low sintering temperature were successfully prepared.

## 2. Experimental section

LMZTF ( $0.02 \leq x \leq 0.08$ ) ceramics were fabricated using  $\text{Li}_2\text{CO}_3$ ,  $\text{MgO}$ ,  $\text{TiO}_2$ ,  $\text{LiF}$ , and  $\text{ZnO}$  as raw materials. The raw materials were mixed with  $\text{ZrO}_2$  balls and deionized water, and the ball-milling time was 8 h. After drying and sieving, all mixtures were pre-fired at  $700^\circ\text{C}$  for 4 h. Then, the calcined powders were ball-milling again for 8 h. After drying and sieving, the paraffin wax was added to the powder for granulation, which was pressed into a cylindrical body of  $\Phi 10 \text{ mm} \times 5 \text{ mm}$ . Finally, these LMZTF samples were sintered at  $850\text{--}975^\circ\text{C}$ .

In this paper, the X-ray diffractometer (Rigaku D/max 2550 PCX) produced in Japan was used to test the phase composition of LMZTF ceramics. A scanning electron microscope (ZEISS MERLIN Compact, Germany) was used to observe the surface microstructure. The Agilent N5234A vector network analyzer was used to measure the dielectric constant and  $Q \times f$  values of LMZTF ceramics. The  $\tau_f$  was calculated according to Eq. (1):

$$\tau_f = \frac{f_2 - f_1}{f_1(T_2 - T_1)} \times 10^6 (\text{ppm}/^\circ\text{C}) \quad (1)$$

where  $f_2$  and  $f_1$  were the resonant frequencies at  $T_2$  ( $85^\circ\text{C}$ ) and  $T_1$  ( $25^\circ\text{C}$ ), respectively.

Fukuda et al. [26] studied the variation law of the temperature coefficient of the resonance frequency of the  $\text{TiO}_2\text{-Bi}_2\text{O}_3$  composite system, and proposed that  $\tau_f$  could be expressed by the following mixing rule:

$$\tau_f = \nu_1 \tau_{f1} + \nu_2 \tau_{f2} \quad (2)$$

where  $\nu_1$  and  $\nu_2$  are the volume fractions of each component, respectively.  $\tau_{f1}$  and  $\tau_{f2}$  are the temperature coefficients of the resonance frequency of each component, respectively.

The bulk densities were measured by the Archimedes method. The theoretical density was obtained by Eq. (3):

$$\rho_{\text{theory}} = \frac{ZA}{V_c N_A} \quad (3)$$

where  $Z$ ,  $A$ ,  $V_c$ , and  $N_A$  were the number of atoms in the unit cell, atomic weight (g/mol), the volume of the unit cell ( $\text{cm}^3$ ), and Avogadro constant ( $\text{mol}^{-1}$ ), respectively. The relative density was obtained as the following formula:

$$\rho_{\text{relative}} = \frac{\rho_{\text{bulk}}}{\rho_{\text{theory}}} \quad (4)$$

## 3. Results and discussion

The XRD pattern of LMZTF ceramics sintered at  $950^\circ\text{C}$  for 6 h is shown in Fig. 1. The diffraction peaks of LMZTF ceramics correspond to the  $\text{Li}_2\text{Mg}_3\text{SnO}_6$  (PDF#39-0932) standard card. When  $0.02 \leq x \leq 0.08$ , the second phase  $\text{Zn}_2\text{TiO}_4$  is detected in the samples. The research by Yang et al. [27] showed that when the amount of  $\text{Zn}^{2+}$  ion substitution was greater than 0.02 mol, the second phase was generated in  $\text{Li}_2(\text{Mg}_{1-x}\text{Zn}_x)_3\text{TiO}_6$  ceramics. However, in this study, the  $\text{Zn}_2\text{TiO}_4$  phase appeared when the amount of  $\text{Zn}^{2+}$  ions

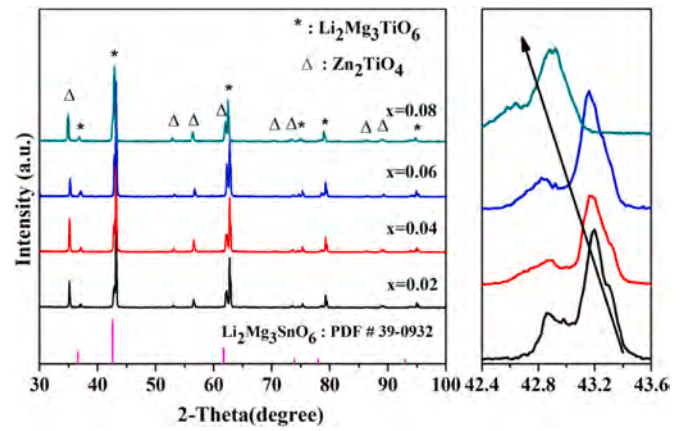


Fig. 1. The XRD patterns of LMZTF ceramics sintered at  $950^\circ\text{C}$  for 6 h.

substitution was greater than or equal to 0.02 mol. It is shown that the substitution of  $\text{F}^-$  ions affect the solid solubility of  $\text{Li}_2\text{Mg}_3\text{TiO}_6$  ceramics. As shown in Fig. 1, the main peaks of LMZTF shift slightly to the lower angle because of the difference in ionic radius between  $\text{Zn}^{2+}$  ion ( $0.740 \text{ \AA}$ ) and  $\text{Mg}^{2+}$  ion ( $0.720 \text{ \AA}$ ).

The microstructure of LMZTF ceramics sintered at  $950^\circ\text{C}$  for 6 h is shown in Fig. 2. To characterize the influence of  $\text{Zn}^{2+}$  substitution on the grain size of LMZTF ceramics, the grain size distribution histograms of sintered samples with different  $x$  values are shown in Fig. 3. When  $x = 0.02$ , the sample surface is dense and uniform. When  $0.04 \leq x \leq 0.08$ , the grain size of the sample is not compact and uniform, and there are fine pores. In general, material composition and sintering temperature affect the microstructure and porosity of ceramics. All the components in Fig. 2 exhibit similar polygonal grains with clear grain boundaries. Compared with SEM images of Zhang et al. [25] on  $\text{Li}_2\text{Mg}_3\text{Ti}(\text{O}_{0.94}\text{F}_{0.08})_6$  ceramics,  $\text{Zn}^{2+}$  ions increase the grain size of ceramics. The average grain sizes are 2.16, 2.36, 2.28, and  $2.35 \mu\text{m}$ , respectively. This may be because the addition of  $\text{Zn}^{2+}$  ions to the grain of  $\text{Li}_2\text{Mg}_3\text{Ti}(\text{O}_{0.94}\text{F}_{0.08})_6$  ceramics weakens the free energy and promotes the grain growth of LMZTF ceramics.

The dispersion degree of particle size distribution is used to test the uniformity of particle size. The formula in the reference

$$\bar{S} = \frac{1}{n} \sum_{i=1}^n S_i \quad (5)$$

$$\sigma = \sqrt{\frac{\sum_{i=1}^n (S_i - \bar{S})^2}{n}} \quad (6)$$

where  $\bar{S}$  and  $\sigma$  are average particle size and dispersion degree of particle size distribution, respectively. Fig. 4 shows the average particle size area and dispersion degree of particle size distribution respectively. From 0.02 to 0.04, the average particle size area increases with the increase of  $\text{Zn}^{2+}$  content. When  $x = 0.02$ , the value is about  $3.664 \mu\text{m}^2$ . When  $x = 0.04$ , the value is about  $4.374 \mu\text{m}^2$ . When  $x = 0.06$ , the value is about  $4.083 \mu\text{m}^2$ . When  $x = 0.08$ , the value is about  $4.374 \mu\text{m}^2$ . When  $x = 0.02$ , the particle size dispersion is the smallest, and when  $x = 0.08$ , the maximum particle size dispersion is

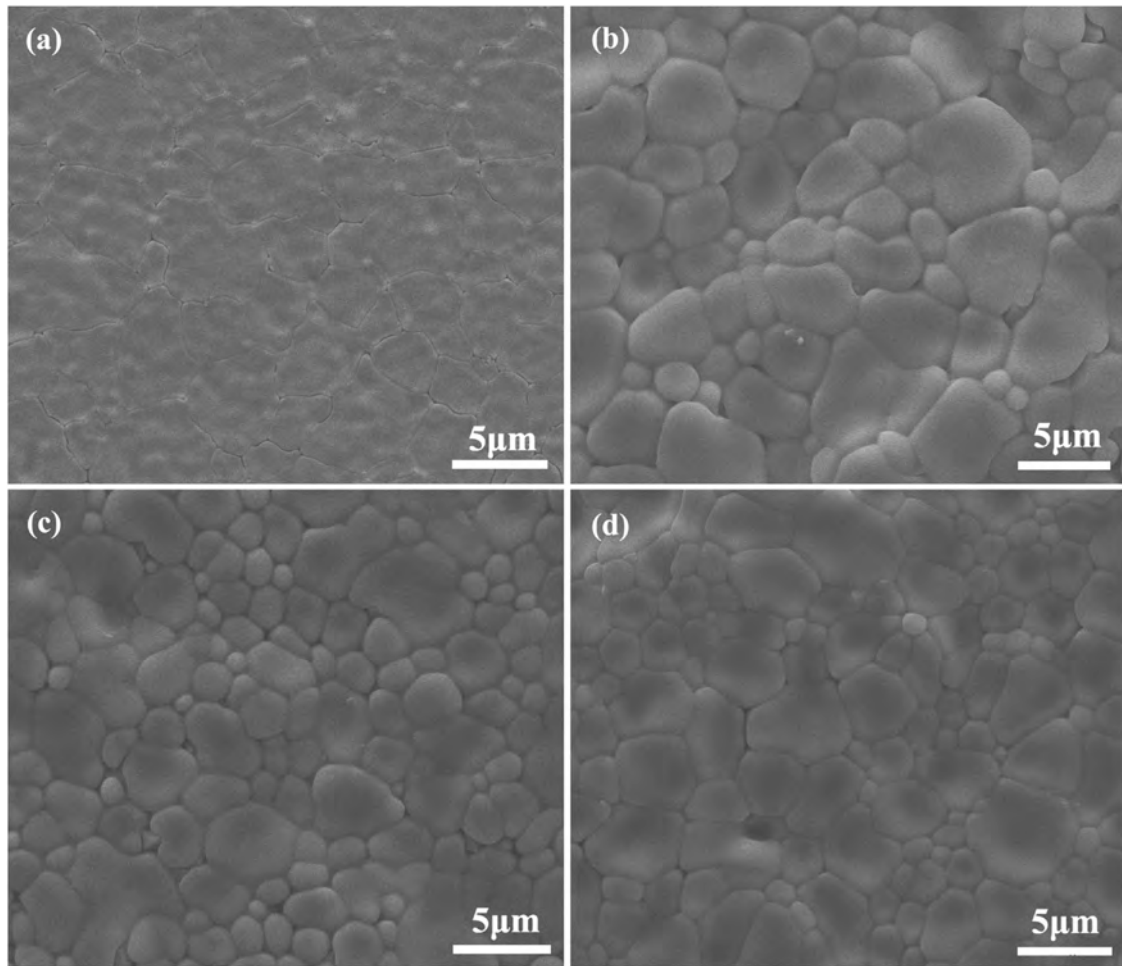


**Fig. 2.** The surface microstructures of LMZTF ceramics sintered at 950 °C for 6 h: (a)  $x = 0.02$ ; (b)  $x = 0.04$ ; (c)  $x = 0.06$ ; (d)  $x = 0.08$ .

obtained, indicating that as the value of  $x$  increases, the particle size distribution gradually becomes uneven.

Fig. 5(a) is the change curve of the relative density of LMZTF ceramics at different sintering temperatures. Overall, the relative density of LMZTF ceramics shows a trend of increasing first and then decreasing with the increase of sintering temperature. In addition, the relative density of LMZTF ceramics reaches a maximum of 95.3% at  $x = 0.02$ , and it declines with the increase of  $x$ . The change of the lattice structure weakens the free energy of LMZTF ceramics and facilitates the sintering process, so the sample has a high degree of densification. When  $0.04 \leq x \leq 0.08$ , the point defects generated by excessive  $\text{Zn}^{2+}$  ions are converted into line defects and surface defects during the sintering process, which affects the density of the LMZTF ceramics, so the density gradually decreases [28].

The dielectric constant of LMZTF ceramics is illustrated in Fig. 5(b). The  $\epsilon_r$  increases rapidly with the sintering temperature rising, which is similar to the tendency of relative densities. The  $\epsilon_r$  of the LMZTF ceramics gradually increases, reaching the maximum value at 950 °C, and then gradually decreases. However, the  $\epsilon_r$  of LMZTF ceramics increases with the increase of doping amount when the sintering temperature is 950 °C, which is opposite to the

changing trend of relative density. This result is mainly caused by the formation of the second phase. It can be known from the XRD pattern that when  $x \geq 0.02$ , the  $\text{Zn}_2\text{TiO}_4$  phase is detected in the sample, indicating that the sample is a multi-phase composite. For heterogeneous composite ceramic materials, the dielectric constant depends on the combination of the volume fraction of the component materials and the dielectric constants of the component materials [29], which can be derived from the following mixing rules [30]:

$$\ln \epsilon = \sum_i V_i \ln \epsilon_i \quad (7)$$

where  $\epsilon_i$  and  $V_i$  are the dielectric constant and volume fraction of the  $i$ -th phase, respectively. The dielectric constant of  $\text{Zn}_2\text{TiO}_4$  is higher than that of  $\text{Li}_2\text{Mg}_3\text{Ti}(\text{O}_{0.96}\text{F}_{0.08})_6$ , so the dielectric constant of LMZTF ceramics gradually increases with the increase of  $x$ .

Fig. 5(c) is the changing trend of  $Q \times f$  values of LMZTF ceramics at different sintering temperatures. The  $Q \times f$  value of LMZTF ceramics reaches its maximum value at 950 °C as the temperature increases. Besides, at 950 °C, the quality factor of LMZTF ceramics is between 115,000 GHz and 128,000 GHz, and the maximum value of

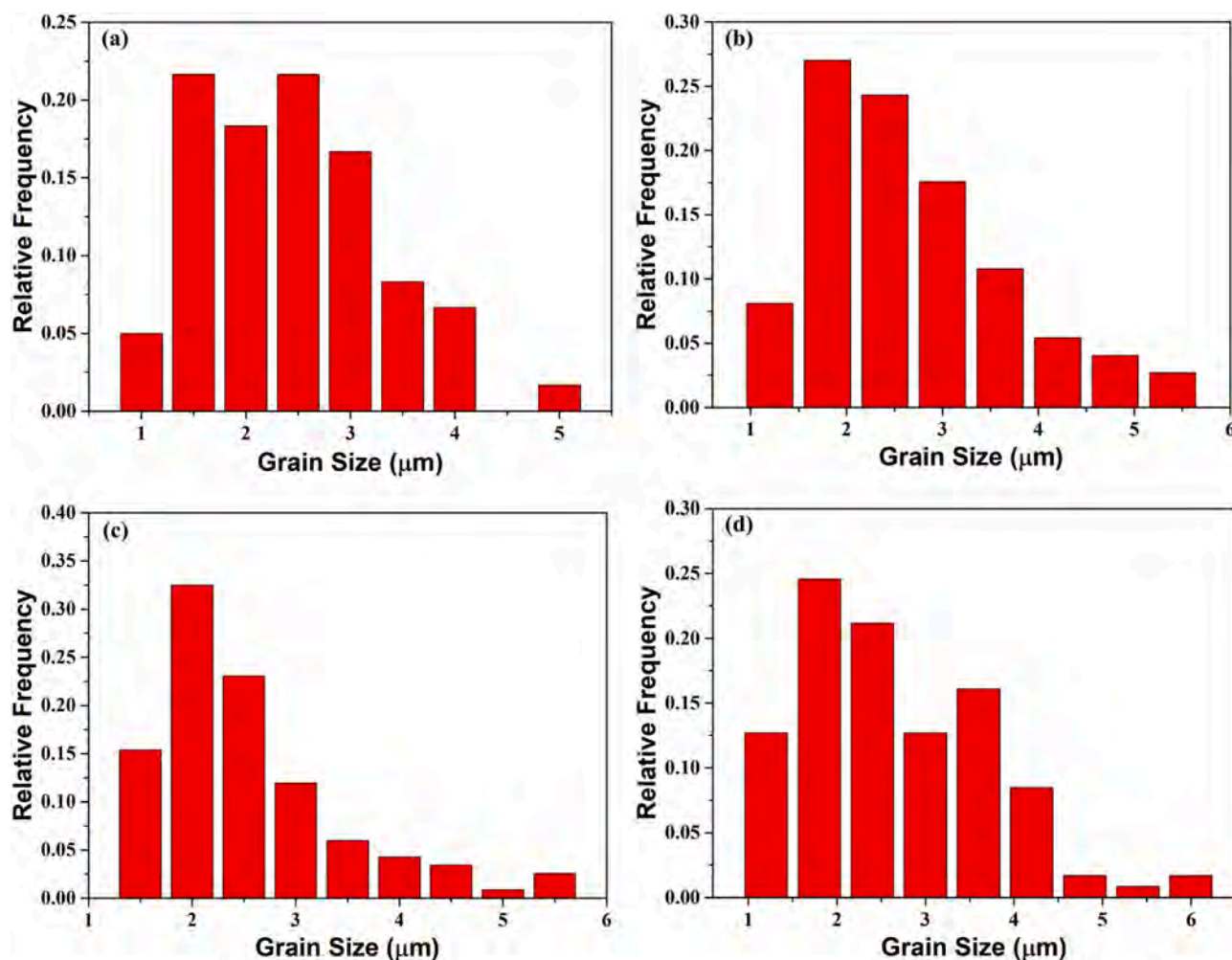


Fig. 3. Grain size distribution of LMZTF ceramics sintered at 950 °C for 6 h: (a)  $x = 0.02$ ; (b)  $x = 0.04$ ; (c)  $x = 0.06$ ; (d)  $x = 0.08$ .

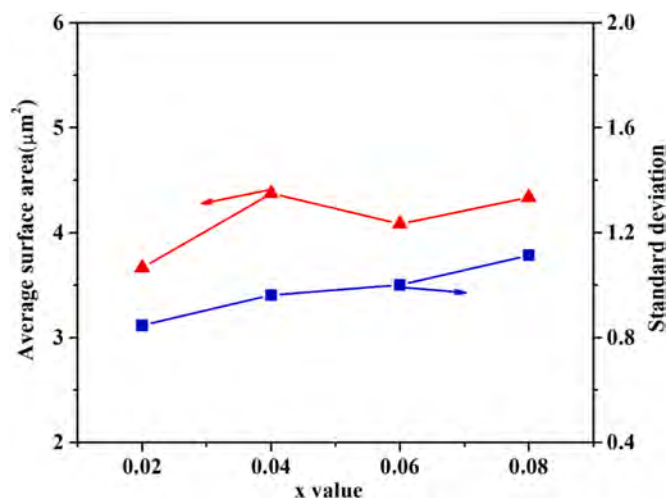


Fig. 4. The average surface area and dispersion degree of particle size sintering at 950 °C for 6 h.

128,000 GHz is obtained at  $x = 0.02$ . The relative density and second phase affect the  $Q \times f$  values greatly. The research results show that the substitution of  $\text{Zn}^{2+}$  effectively improves the  $Q \times f$  value of  $\text{Li}_2\text{Mg}_3\text{Ti}(\text{O}_{0.94}\text{F}_{0.08})_6$  ceramics. This is because the substitution of  $\text{Zn}^{2+}$  ions causes lattice distortion and introduces point defects to promote sintering and obtain a larger bulk density. Also, the decrease in  $Q \times f$  values when the amount of  $\text{Zn}^{2+}$  substitution is greater than 0.02 mol is due to the increase of the content of the second phase  $\text{Zn}_2\text{TiO}_4$ . The quality factor of  $\text{Zn}_2\text{TiO}_4$  is about 1000–2000 GHz, which will reduce the  $Q \times f$  value of  $\text{Li}_2\text{Mg}_3\text{Ti}(\text{O}_{0.94}\text{F}_{0.08})_6$  ceramics.

The  $\tau_f$  values of LMZTF ceramics sintered at 950 °C for 6 h are shown in Fig. 6. We observe that due to the small distinction between the temperature coefficient of  $\text{Li}_2\text{Mg}_3\text{TiO}_6$  ceramics and  $\text{Zn}_2\text{TiO}_4$  ceramics, the  $\tau_f$  of  $\text{Li}_2\text{Mg}_3\text{TiO}_6$  ceramics changes slightly with the increase of  $\text{Zn}^{2+}$  content ( $\text{Li}_2\text{Mg}_3\text{TiO}_6$ :  $-39 \text{ ppm}/^\circ\text{C}$ ;  $\text{Zn}_2\text{TiO}_4$ :  $-67 \text{ ppm}/^\circ\text{C}$ ). The dielectric properties of LMZTF ceramics are shown in Table 1. It can be concluded that  $\text{Li}_2(\text{Mg}_{0.98}\text{Zn}_{0.02})_3\text{Ti}(\text{O}_{0.96}\text{F}_{0.08})_6$  ceramic has the largest relative density and high performance:  $\epsilon_r \sim 14.64$ ,  $Q \times f \sim 128,000 \text{ GHz}$ ,  $\tau_f \sim -33.9 \text{ ppm}/^\circ\text{C}$ .

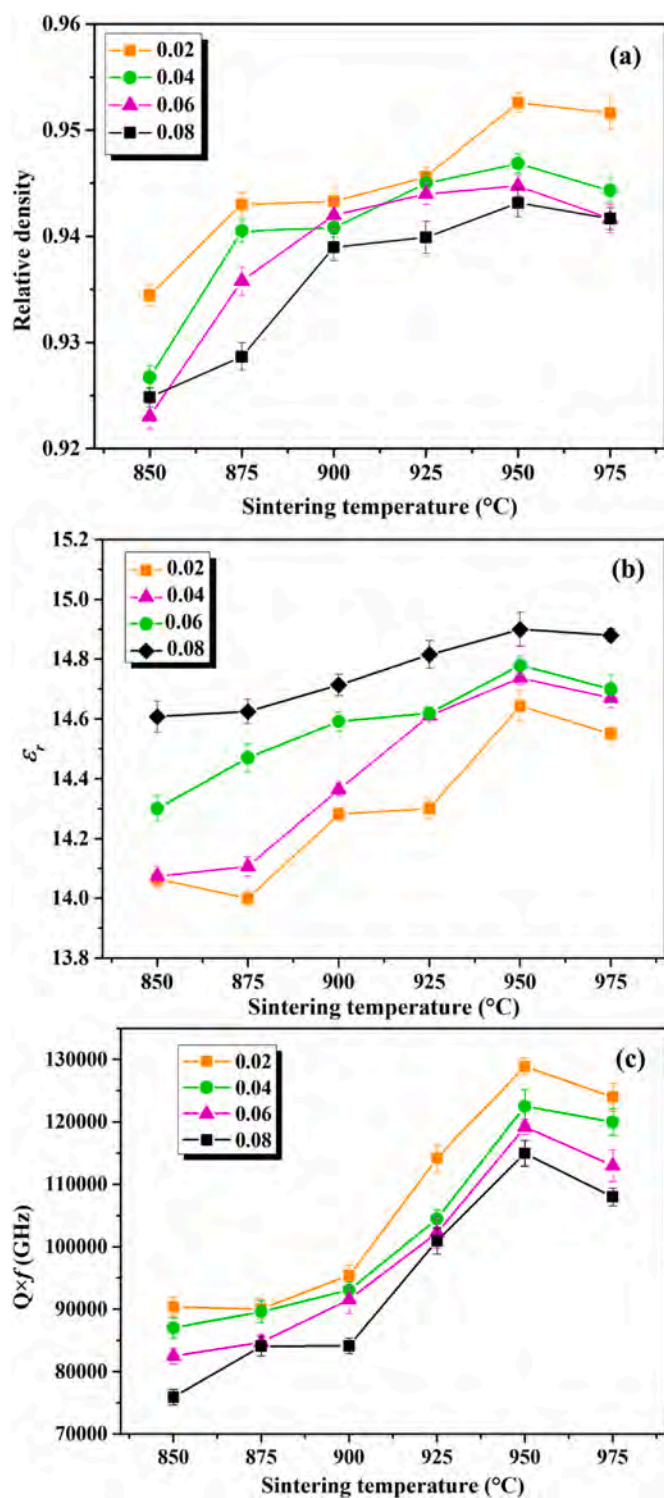


Fig. 5. The variations in relative density, dielectric constant, and  $Q \times f$  values of LMZTF ceramics sintered at various temperature for 6 h as a function of  $Zn^{2+}$  ions content.

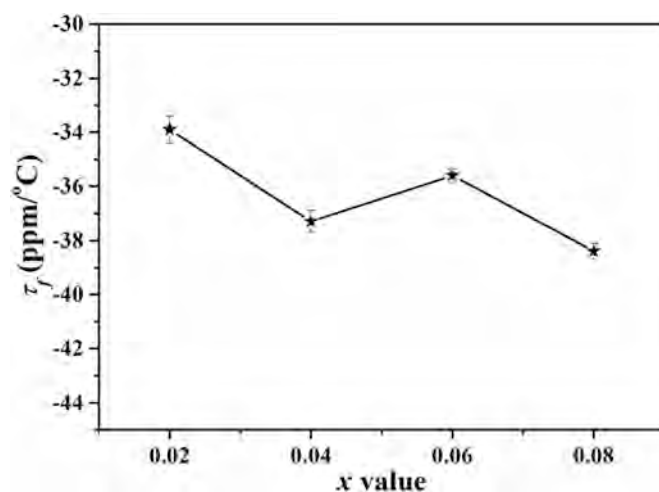


Fig. 6. The  $\tau_f$  values of LMZTF ceramics sintered at 950 °C for 6 h.

Table 1

Relative density and microwave dielectric properties of LMZTF ceramics sintered at 950 °C.

LMZTF	Relative density (%)	$\epsilon_r$	$Q \times f$ (GHz)	$\tau_f$ (ppm/°C)
$x = 0.02$	95.2	14.64	128,000	-33.9
$x = 0.04$	94.6	14.73	122,000	-37.3
$x = 0.06$	94.4	14.78	119,000	-35.6
$x = 0.08$	94.3	14.9	115,000	-38.4

#### 4. Conclusions

In this work, when  $x = 0.02$ , the substitution of  $Zn^{2+}$  ions reduced the free energy, promoted the sintering process, and obtained optimal relative density value and dielectric properties. When  $0.04 \leq x \leq 0.08$ , the increase of the content of the second phase  $Zn_2TiO_4$  had a certain adverse impact on the density and performance. In summary, this paper showed that the  $Q \times f$  values of  $Li_2Mg_3Ti(O_{0.96}F_{0.08})_6$  ceramics could be improved through ion doping. Particularly, when the sintering temperature is 950 °C,  $Li_2(Mg_{0.98}Zn_{0.02})_3Ti(O_{0.96}F_{0.08})_6$  ceramic has the best dielectric properties:  $\epsilon_r \sim 14.64$ ,  $Q \times f \sim 128,000$  GHz,  $\tau_f \sim -33.9$  ppm/°C.

#### CRediT authorship contribution statement

**Ping Zhang:** Conceptualization, Methodology, Validation, Investigation, Writing-original draft, Writing-review & editing, Resources. **Manman Hao:** Methodology, Validation, Writing-original draft, Formal analysis, Data curation, Software. **Xin Tian:** Data curation. **Sheng Xie:** Methodology, Validation, Resources.

#### Declaration of Competing Interest

The authors declare that they have no known competing financial interests or personal relationships that could have appeared to influence the work reported in this paper.

## Acknowledgements

This work was supported by Major Projects of Science and Technology in Tianjin, China (No. 18ZXJMTG00020).

## References

- [1] D. Thomas, M.T. Sebastian, Temperature-compensated  $\text{LiMgPO}_4$ : a new glass-free low-temperature cofired ceramic, *J. Am. Ceram. Soc.* 93 (2010) 3828–3831.
- [2] I.M. Reaney, D. Iddles, Microwave dielectric ceramics for resonators and filters in mobile phone networks, *J. Am. Ceram. Soc.* 89 (2006) 2063–2072.
- [3] A.T. Vanderah, Talking ceramics, *Science* 298 (2002) 1182–1184.
- [4] W.S. Xia, L.Y. Zhang, Y. Wang, J.T. Zhang, R.R. Feng, L.W. Shi, Optimized sintering properties and temperature stability of  $\text{MgZrTa}_2\text{O}_8$  ceramics with CuO addition for microwave application, *J. Mater. Sci. Mater. Electron.* 28 (2017) 18437–18441.
- [5] J.Y. Deng, W.S. Xia, W.H. Zhang, T.L. Tang, Y. Wang, J.L. Du, Optimization of sintering behavior and microwave dielectric properties of  $\text{LaNbO}_4$  ceramics with NiO/CoO additive, *J. Alloy. Compd.* 859 (2021) 158378.
- [6] M.T. Sebastian, H. Jantunen, Low loss dielectric materials for LTCC applications: a review, *Int. Mater. Rev.* 53 (2008) 57–90.
- [7] Z. Fu, J. Ma, X. Zhang, B. Wang, The effect of sintering agents on the sinterability and dielectric properties of  $\text{Li}_2\text{Mg}_3\text{TiO}_6$  ceramics, *Ferroelectrics* 510 (2017) 50–55.
- [8] J. Ma, Z. Fu, P. Liu, L. Zhao, B. Guo, Ultralow-fired  $\text{Li}_2\text{Mg}_3\text{TiO}_6\text{-Ca}_{0.8}\text{Sr}_{0.2}\text{TiO}_3$  composite ceramics with temperature stable at microwave frequency, *J. Alloy. Compd.* 709 (2017) 299–303.
- [9] Y.D. Zhang, D. Zhou, Pseudo phase diagram and microwave dielectric properties of  $\text{Li}_2\text{O-MgO-TiO}_2$  ternary system, *J. Am. Ceram. Soc.* 99 (2016) 3643–3650.
- [10] H.F. Zhou, X.H. Tan, J. Huang, X.L. Chen, Sintering behavior, phase evolution and microwave dielectric properties of thermally stable  $\text{Li}_2\text{O-3MgO-mTiO}_2$  ceramics ( $1 \leq m \leq 6$ ), *Ceram. Int.* 43 (2017) 3688–3692.
- [11] T. Xie, L. Zhang, H. Ren, M. Dang, H. Wang, S. Jiang, X. Zhao, F. Meng, H. Lin, L. Luo, A novel temperature-stable and low-loss microwave dielectric using  $\text{Ca}_{0.8}\text{Sr}_{0.2}\text{TiO}_3$ -modified  $\text{Li}_2\text{Mg}_3\text{TiO}_6$  ceramics, *J. Mater. Sci. Mater. Electron.* 28 (2017) 13705–13709.
- [12] G.G. Yao, X.S. Hua, X.L. Tian, P. Liu, J.P. Zhou, Synthesis and microwave dielectric properties of  $\text{Li}_2\text{MgTiO}_4$  ceramics, *Ceram. Int.* 41 (2015) S563–S566.
- [13] S. George, M.T. Sebastian, Synthesis and microwave dielectric properties of novel temperature stable high Q,  $\text{Li}_2\text{ATi}_3\text{O}_8$  (A = Mg, Zn) ceramics: rapid communications of the american ceramic society, *J. Am. Ceram. Soc.* 93 (2010) 2164–2166.
- [14] Z.F. Fu, P. Liu, J.L. Ma, X.G. Zhao, H.W. Zhang, Novel series of ultra-low loss microwave dielectric ceramics:  $\text{Li}_2\text{Mg}_3\text{BO}_6$  (B = Ti, Sn, Zr), *J. Eur. Ceram. Soc.* 36 (2015) 625–629.
- [15] P. Zhang, H. Xie, Y.G. Zhao, M. Xiao, Microwave dielectric properties of low loss  $\text{Li}_2(\text{Mg}_{0.95}\text{A}_{0.05})_3\text{TiO}_6$  (A =  $\text{Ca}^{2+}$ ,  $\text{Ni}^{2+}$ ,  $\text{Zn}^{2+}$ ,  $\text{Mn}^{2+}$ ) ceramics system, *J. Alloy. Compd.* 689 (2016) 246–249.
- [16] P. Zhang, H. Xie, Y.G. Zhao, M. Xiao, Synthesis and microwave dielectric characteristics of high-Q  $\text{Li}_2\text{Mg}_x\text{TiO}_{3+x}$  ceramics system, *Mater. Res. Bull.* 98 (2018) 160–165.
- [17] H.L. Pan, L. Cheng, H.T. Wu, Relationship between crystal structure and microwave dielectric properties of  $\text{Li}_2(\text{Mg}_{1-x}\text{Co}_x)_3\text{TiO}_6$  ( $0 \leq x \leq 0.4$ ) ceramics, *Ceram. Int.* 43 (2017) 15018–15026.
- [18] H.L. Pan, Y.W. Zhang, H.T. Wu, Crystal structure, infrared spectroscopy and microwave dielectric properties of ultra low-loss  $\text{Li}_2\text{Mg}_3\text{Ti}_{0.95}(\text{Mg}_{1/3}\text{Sb}_{2/3})_{0.05}\text{O}_6$  ceramic, *Ceram. Int.* 44 (2018) 3464–3468.
- [19] Y.K. Yang, H.L. Pan, H.T. Wu, Crystal structure, Raman spectra and microwave dielectric properties of  $\text{Li}_2\text{Mg}_3\text{Ti}_{0.95}(\text{Mg}_{1/3}\text{Nb}_{2/3})_{0.05}\text{O}_6$  ceramic, *Ceram. Int.* 44 (2018) 11350–11356.
- [20] J.L. Ma, Z.F. Fu, P. Liu, L.P. Zhao, B.C. Guo, Ultralow-fired  $\text{Li}_2\text{Mg}_3\text{TiO}_6\text{-Ca}_{0.8}\text{Sr}_{0.2}\text{TiO}_3$  composite ceramics with temperature stable at microwave frequency, *J. Alloy. Compd.* 709 (2017) 299–303.
- [21] H.L. Pan, M.T. Liu, M.F. Li, F. Ling, H.T. Wu, Low temperature sintering and microwave dielectric properties of  $\text{Li}_5\text{Mg}_7\text{Ti}_3\text{O}_{16}$  ceramics with LiF additive for LTCC applications, *J. Mater. Sci. Mater. Electron.* 29 (2018) 999–1003.
- [22] R.Z. Zuo, J. Zhang, J. Song, Y.D. Xu, Liquid-phase sintering, microstructural evolution, and microwave dielectric properties of  $\text{Li}_2\text{Mg}_3\text{SnO}_6\text{-LiF}$  ceramics, *J. Am. Ceram. Soc.* 101 (2018) 569–576.
- [23] Z.F. Fu, P. Liu, J.L. Ma, X.M. Chen, H.W. Zhang, New high Q low-fired  $\text{Li}_2\text{Mg}_3\text{TiO}_6$  microwave dielectric ceramics with rock salt structure, *Mater. Lett.* 164 (2016) 436–439.
- [24] A. Ullah, H.X. Liu, H. Hao, J. Iqbal, Z.H. Yao, M.H. Cao, Q. Xu, Effect of Zn substitution on the sintering temperature and microwave dielectric properties of  $\text{MgSiO}_3$ -based ceramics, *Ceram. Int.* 43 (2017) 484–490.
- [25] P. Zhang, M.M. Yang, M. Xiao, Z.T. Zheng, Sintering behavior and microwave dielectric properties of  $\text{Li}_2\text{Mg}_3\text{Ti}(\text{O}_{1-x/2}\text{F}_x)_6$  ( $0.06 \leq x \leq 0.15$ ) ceramics for LTCC application, *Mater. Chem. Phys.* 236 (2019) 121805.
- [26] K. Fukuda, R. Kitoh, I. Awai, Microwave characteristics of  $\text{TiO}_2\text{-Bi}_2\text{O}_3$  dielectric resonator, *Jpn. J. Appl. Phys.* 32 (1993) 4584–4588.
- [27] C.H. Yang, H.L. Pan, Y.K. Yang, H.T. Wu, Influence of Zn substitution on the crystal structures and microwave dielectric properties of  $\text{Li}_2(\text{Mg}_{1-x}\text{Zn}_x)_3\text{TiO}_6$  ( $0 \leq x \leq 0.2$ ) ceramics, *Ceram. Int.* 764 (2018) 424–430.
- [28] Y. Hao, Q. Zhang, J. Zhang, C.R. Xin, H. Yang, Enhanced sintering characteristics and microwave dielectric properties of  $\text{Li}_2\text{TiO}_3$  due to nano-size and non-stoichiometry effect, *J. Mater. Sci.* 22 (2012) 23885–23892.
- [29] S.J. Perm, N.M. Alford, A. Templeton, X.R. Wang, M.S. Xu, M. Reece, K. Schrapel, Effect of porosity and grain size on the microwave dielectric properties of sintered alumina, *J. Am. Chem. Soc.* 80 (1997) 1885–1888.
- [30] R.D. Shannon, G.R. Rossman, Dielectric constants of silicate garnets and the oxide additivity rule, *Am. Mineral.* 77 (1992) 94–100.